Photodissociation Dynamics of Heteronuclear Diatomic Ion (ICl^-) in a Linear-Chain Model

Jaejin Ka and Seokmin Shin*

Department of Chemistry and Center for Molecular Catalysis, Seoul National University, Seoul 151-742, Korea

Received: January 16, 1998; In Final Form: March 18, 1998

Photodissociation and recombination dynamics of ICl^- in condensed-phase environments is studied theoretically by a linear-chain model consisting of a diatom in a chain of rare-gas atoms. We use a hybrid quantum/classical scheme, where the dynamics of the solute is treated by time-dependent quantum mechanics, while the motions of the solvent atoms are described classically. The dynamics of the heteronuclear diatomic ion, ICl^-, is much more complex compared with those for the homonuclear (I_2^-) case. The photodissociation dynamics of the model system $|(Ar)_{50}[Cl-I]^-(Ar)_{50}|$ show very fast initial recombination due to the motion of the lighter Cl atom. The mass asymmetry in ICl^- is found to have a strong influence on the detailed kinematics of the system such as the solvent dependence of the energy transfer and the movement of the center of mass of the diatom. To examine the effects on the dynamics by the structural changes in the solvents, we considered variations of the linear-chain model such as the one-sided chain model $(Ar)_{50}[Cl-I]^-$ and the linear cluster model $(Ar)_5[Cl-I]^-(Ar)_5$.

1. Introduction

Dynamics involved in a chemical reaction can be affected by the properties of the solvent, more so for the reactions of the charged species.[1] Photodissociation of a diatom in condensed phases such as large molecular clusters, solid matrixes, and liquids has revealed various aspects of the solvent influence on the course of a chemical reaction.[2] Although the general features of photodissociation and recombination in condensed phases are rather well established, there are several issues unresolved concerning detailed microscopic pictures for the processes involved. Of particular interest is the role of electrostatic interactions on solution/cluster reaction dynamics. Time-resolved experiments on the photodissociation and recombination dynamics of I_2^- in several solvents such as water or alcohols have been done.[3−5] One of the main observations is a very fast vibrational relaxation rate of the charged solute in polar solvents compared with the case of neutral molecule (I_2) in nonpolar solvents. It is partly attributed to the strong electrostatic forces arising from the shifting charge distribution as shown in a molecular dynamics simulation based on nonequilibrium free energy functions.[6]

Recently, Lineberger et al. have done systematic studies of solvent-mediated reactions in molecular cluster ions to examine the stepwise effect of increasing solvation on electronic structure and reactivity.[7−11] New experimental techniques, such as ultrafast laser spectroscopy for probing the reaction dynamics on extremely short time scales along with the mass spectrometry for selecting well-characterized solvent environments, have proven useful in such studies. In the early experiments, the time-dependent cage effect in $I_2^-(CO_2)_n$ cluster ions as a function of cluster size following 720 nm excitation has been reported.[7−9] Geminate recombination rates exhibit strong cluster size dependence in the range $n = 13-15$. Absorption recovery times for $I_2^-(CO_2)_n$ were ∼30 ps for the smaller precursor size range and ∼10 ps for the larger range. Both Monte Carlo simulations[12] and experiments indicate that 16 CO_2 molecules constitute the first solvent shell around I_2^-. A recurrence in the absorption recovery at early times was interpreted to result from the coherent motion of the caged fragments on the excited states.[8]

Several experimental and theoretical studies of I_2^- clustered with simpler solvent Ar have provided much more detailed information about ultrafast reaction dynamics in the photodissociation of the molecular cluster ions. Vorsa et al. have studied the photodissociation of $I_2^-(Ar)_n$ clusters with $n = 1-27$.[10] The relative abundance of recombined products increases smoothly but rapidly with the number n of argon atoms in the precursor cluster, reaching 100% in clusters having less than a single solvent shell around the ion. From the femtosecond pump−probe experiment, which examines the reappearance of I_2^- near the bottom of the ground-state well, they found that the time scale for the overall process is much larger than the absorption recovery time for the system $I_2^-(CO_2)_n$.[11] The experiments by Vorsa et al. and the anion femtosecond photoelectron spectroscopy study by Greenblatt et al.[13] have indicated that photodissociation of the larger cluster $I_2^-(Ar)_n$ results in caging of the I_2^- followed by recombination and vibrational relaxation on both the excited and the ground electronic states. Recent theoretical studies of similar systems by using nonadiabatic molecular dynamics simulations have generally confirmed the main findings of the experiments.[14−16]

Photofragmentation studies of $ICl^-(CO_2)_n$ cluster ions have also been done by Lineberger et al.[17] A primary motivation for such studies is to investigate the effects of the solvent on the charge distribution in a heteronuclear chromophore and to compare it with a homonuclear ionic chromophore solvated by the same number of solvent molecules. Photodissociation in $ICl^-(CO_2)_n$ clusters with a partially complete solvation shell is considerably more complex because of the initial asymmetric solvent distribution between the I and Cl atoms. Owing to its smaller size and larger electron affinity, the Cl end of the

---

* To whom correspondence should be addressed. Telephone: 82-2-880-6639. Fax: 82-2-889-1568. E-mail: sshin@plaza.snu.ac.kr.

S1089-5639(98)00798-1 CCC: $15.00

diatomic anion will be preferentially solvated, and therefore, the first solvent molecules cluster about the Cl end of the diatom. This preferential solvation of the Cl atom enhances the slight asymmetry in the initial charge distribution in the bare ion. Following photoexcitation nominally correlating to the I$^-$-based direct photofragment, a solvent-induced recombination is observed to form ICl$^-$, and a solvated Cl$^-$-based product is also observed. The two new product channels are the results of nonadiabatic transitions. The Cl$^-$ products must result from charge transfer from I$^-$ to Cl within the disintegrating complex. The relative importance of the different photofragment channels strongly depends on the cluster ion size. An ICl$^-$ caged product is first observed for ICl$^-$(CO$_2$)$_2$, increasing rapidly to a maximum at $n \approx 6$ and then decreasing. Such caging efficiency is dramatically different from that of I$_2^-$(CO$_2$)$_n$ cluster ions. The Cl$^-$ photofragment channel increases smoothly for the cluster size range studied and becomes the dominant channel for $n \approx 8$. The relative yields of the ICl$^-$- and Cl$^-$-based products reflect the extent to which solvation influences the photodissociation pathways of ICl$^-$.

The difference between the dissociation dynamics of ICl$^-$ and I$_2^-$ can also be understood in terms of the kinematics. Owing to the mass asymmetry, the lighter Cl fragment carries away much of the kinetic energy released. The Cl end is surrounded by the solvent molecules with roughly the same mass, providing an efficient energy-transfer mechanism and thereby enhancing recombination. In ICl$^-$(CO$_2$)$_n$ cluster ions, the primary mechanism for the recombination is more likely via the hard wall repulsive interaction with the solvent molecules.

Previously, we have studied photodissociation and recombination dynamics of I$_2^-$ in condensed-phase environments by a linear-chain model consisting of a diatom in a chain of rare-gas atoms.[18] We used a hybrid quantum/classical method, in which the wave packet dynamics of I$_2^-$ is treated quantum mechanically while the solvent atoms are described classically. Rapid recombination and subsequent solvent-induced coherent vibrations are observed when the mass of the solvent atom is comparable to that of the solute. The effects of the solvents on the electronic structure of the diatomic ion is modeled by introducing an effective solvent field representing the change in solvent polarization. The gas-phase potential energy surfaces are modified by the presence of the solvent field, which can lead to a charge switching and nonadiabatic transitions. The solvent field is based on a one-electron picture,[12,19−21] which is widely used to describe charge-transfer processes in various systems.[22,23]

In this study, we investigated the photodissociation of ICl$^-$ in a linear-chain model. As mentioned before, the dynamics of the heteronuclear diatomic ion (ICl$^-$) is much more complex compared with those for the homonuclear case (I$_2^-$). One can think of three factors contributing to the differences: gas-phase electronic structure, interaction with solvent atoms, and mass asymmetry in ICl$^-$. The present model, albeit simple, is expected to provide qualitatively correct pictures for the dynamical effects resulting from the differences in the potential energy surfaces and the mass asymmetry. The hard repulsive walls of solvents, which are primary mechanism for the recombination of ICl$^-$, are well represented in the model. The effects of the electrostatic interactions including the initial charge asymmetry in ICl$^-$ molecule can be partially examined by using the solvent field model. To study the influence on the dynamics by the structural changes in the solvents, we considered variations of the linear-chain model such as the one-sided chain model and the linear cluster model.

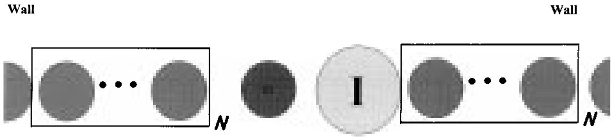

Figure 1. Schematic diagram of linear-chain model for ICl$^-$ embedded in rare-gas matrixes. N represents the number of solvent atoms. In a one-sided chain model, the solvent atoms on the right (I atom) side are missing, while the wall at both ends of the linear chain is removed for a linear cluster model.

The paper is organized as follows. The theoretical models and the computational methods are presented in section 2. Section 3 gives detailed descriptions of the results of the study. The main findings and discussions are summarized in section 4.

2. Theoretical Model

We use a one-dimensional model for the dynamics of photodissociation and recombination of a diatom. The model consists of a single diatom embedded in a symmetrically arranged linear array of rare-gas atoms. In our previous study,[18] the homonuclear I$_2^-$ is assumed to have symmetric motion with the center of mass for the diatom fixed. In the case of ICl$^-$, I and Cl atoms are allowed to move independently. The schematic picture of the model is given in Figure 1. Similar one-dimensional models have been used to obtain general features of the dynamics of photodissociation and the energy-transfer processes.[24−29] The two atoms of the solute are coupled to the two adjacent solvent atoms, and all the solvent atoms are coupled to each adjacent atoms through the Lennard-Jones potential. The last solvent atom at each end of the chain are connected to a static wall. The reflective boundary is not expected to affect short-time dynamics, which is the main interest of the present study.

In the study of cluster ions such as ICl$^-$(CO$_2$)$_n$, the solvent atoms form an asymmetric structure by solvating the Cl side preferably for small n. We have considered the modifications of the linear-chain model to examine such structural characteristics on the dynamics of the solute. First, we introduced a one-sided linear-chain model in which the solvent atoms are present on only one side of the diatom. Second, molecular cluster ions are described by a linear cluster model where the walls at the end of the linear chain are removed and the solvent atoms are allowed to be evaporated.

For the potential energy of the diatom, gas-phase potentials for ICl$^-$ are used.[30] Two electronic states are considered: the ground state and the excited state reached by photoabsorption. The electronic transition responsible for photodissociation is taken to be ${}^2\Sigma^+_{1/2} \rightarrow {}^2\pi_{1/2}$. The potentials are modeled by Morse functions, and the parameters for the Morse potentials are given in Table 1 along with those for the LJ potentials. Figure 2 shows the potential surfaces for ICl$^-$ used in the present study. The corresponding potential surfaces for the homonuclear I$_2^-$ can be found in ref 18.

The effects of the solvents on the electronic structure of a dihalide ion can be considered by a simple one-electron picture.[12,20,21] It is expected that the distribution of the excess charge in ICl$^-$ is mainly determined by the electrostatic potential difference between the two atoms (ΔU), reflecting the asymmetric electrostatic environment due to solvent atoms. A uniform electric field (E) provides a reasonable model of solvation. The strength of the solvent field is determined to

TABLE 1: Parameters of Potential Functions

	Morse parameters[a,b]				
	D (cm^{-1})	r_e (Å)	β (Å^{-1})	ν_e (cm^{-1})	V_0 (cm^{-1})
$I^- + Cl$ ex($^2\Pi_{1/2}$)	1129.24	4.34	0.812	33	4436.3
ICl^- gr($^2\Sigma^+_{1/2}$)	6702.8	2.93	1.41	179.5	0

	Lennard-Jones parameters				
	ϵ (cm^{-1})	σ (Å)		ϵ (cm^{-1})	σ (Å)
$I^{-1}-Ar$	130.24	3.63	$I^{-1}-Xe$	264.4	3.914
$Cl^{-1}-Ar$	105	3.32	$Cl^{-1}-Xe$	159	3.605
$Ar-Ar$	84	3.40	$Xe-Xe$	192	3.97

[a] Reference 30. [b] The Morse function potential has the following form: $V(r) = D\{\exp[-2\beta(r - r_e)] - 2\exp[-\beta(r - r_e)]\}$.

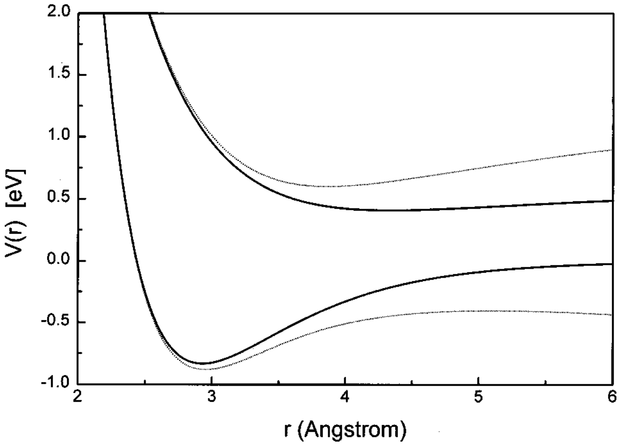

Figure 2. Upper and lower solid lines correspond to the potential curves for the excited ($^2\Sigma^+_{1/2}$) and the ground ($^2\pi_{1/2}$) state of ICl^- involved in the photodissociation. The dotted lines are the corresponding potential curves when the effective solvent field has a value of 0.004 au.

reproduce the potential energy difference, $E = \Delta U/R$ where R is the bond length of the diatom. We are concerned about evaluating potential energy surfaces of the ground and the excited states of ICl^- under the influence of the solvent field. The solvent field can also be defined as the electrostatic field at the center of the diatom exerted by the solvent charges. For the solute charges separated by R, the potential energy difference should be given by $\Delta U = ER$. In the one-electron model, the extra electron feels the potential of the diatom core and the solvent electric field. The electronic structure of the system is determined by the Hamiltonian $H = H_0 + eE\hat{x}$, where H_0 is the Hamiltonian for the isolated anion and the internuclear axis is along the x direction.

The calculations of the potential energy surfaces can be done in the diabatic picture.[6,12,20] In the two electronic state model, the two adiabatic potential energy surfaces can be thought to be obtained by the following diabatic potential matrix:

$$\mathbf{U}_{db} = \begin{pmatrix} \alpha & -\beta \\ -\beta & \alpha \end{pmatrix} \tag{1}$$

which is equivalent to

$$E^0_{gr} = E^0_- = \alpha(r) - \beta(r) \tag{2a}$$

$$E^0_{ex} = E^0_+ = \alpha(r) + \beta(r) \tag{2b}$$

for the ground and the excited states. The diabatic potential energy matrix elements $\alpha(r)$ and $\beta(r)$ can be obtained once the two adiabatic surfaces are known. The two diabatic states can be defined to represent the situations where the extra electron is localized around one side of the diatom. In the absence of the solvent atoms, we take the two diabatic states to be degenerate. When we include the effect of the solvents, the energies of the two diabatic states become different because of the asymmetric solvent configuration in which one side of the diatom is preferentially solvated. In our model, the energy difference is given by eEr in the one-electron picture using the effective solvent field. In the presence of the effective electric field, the diabatic potential becomes[12]

$$\mathbf{U}_{db}(E) = \begin{pmatrix} \alpha - \dfrac{eEr}{2} & -\beta \\ -\beta & \alpha + \dfrac{eEr}{2} \end{pmatrix} \tag{3}$$

where E is the magnitude of constant electric field. The resulting adiabatic potentials are given by

$$E_\pm(E) = \alpha \pm \frac{1}{2}\sqrt{(eEr)^2 + 4\beta^2} \tag{4}$$

We note that the solvent field is a dynamical variable determined by the solvent motions. In the early dynamics after photoexcitation, the solvent configuration can be considered as fixed until the solvent atoms start to respond to a change in the charge distribution. The equilibrium bond length of ICl^- changes under the influence of the solvent field. The changes in PESs by the repulsive interactions of the solvent and the effect of the solvent field are illustrated in Figure 2.

We use a hybrid quantum/classical scheme based on the time-dependent Hartree approximation.[31] The dynamics of the solute (ICl^-) is treated by time-dependent quantum mechanics, while the motions of the solvent atoms are described by classical trajectories. The detailed method has been presented in the previous work.[18] Unlike the homonuclear ($I_2{}^-$) case, the solute ICl^- is represented by separate coordinates for I and Cl atoms. The quantum dynamics of the solute are described by the time-dependent propagation of the two-dimensional wave function in these coordinates. The wave packet propagation is done using a split operator method,[32,33] and the classical dynamics of the solvent atoms are calculated by using the velocity Verlet algorithm.[34]

The wave packet propagation in quantum dynamics is usually done on numerical grids.[35] Fine spatial grids are necessary for better convergence, while the speed of the calculations demands the reduction of the number of grid points. As a result, the range of spatial region represented by the grids is very difficult to be extended. This causes a problem for studying dynamics that involve long-range motions such as dissociation. One solution to the problem is to use the dynamic grids that are defined as moving with the molecular system represented by the grids.[36] In our case, whenever the middle of the wave packets representing I or Cl atoms passes a reference point in the original grid range, new grids are constructed. The center of the new grid system is located at the average position of the wave packet at the time of changing grids, while the range of the grid is not changed, thus keeping the grid spacing constant. Since we are using the same points in the overlap region, the interpolation of the wave function into the new grid is straightforward. The wave function in the nonoverlap region is assumed to be zero. This will not cause much problem if we use a large enough initial grid and control the frequency of the switching of the grids. Fixed grids are used for the dynamics in the linear-chain model, since the range of initial grid can be sufficient for the short-time dynamics we are interested in. For

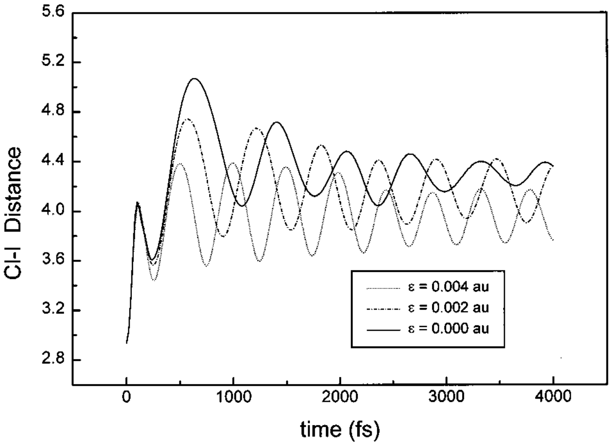

Figure 3. Averaged internuclear Cl−I distance (in Å) as a function of time for the model system $|(Ar)_{50}[Cl-I]^-(Ar)_{50}|$. Three values of the solvent field (0.000, 0.002, and 0.004 au) are used in the calculations.

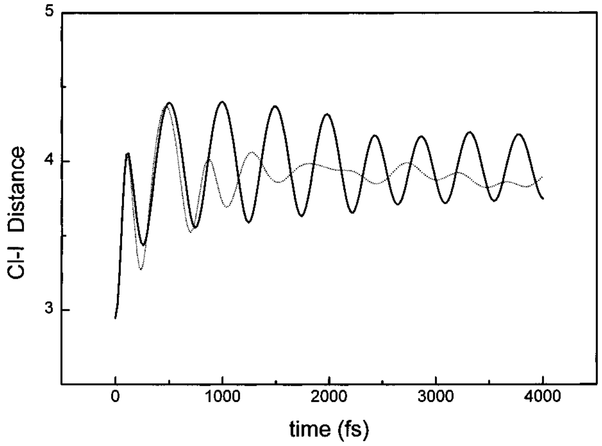

Figure 4. Comparison of the averaged internuclear Cl−I distances (in Å) for the model system $|(Ar)_{50}[Cl-I]^-(Ar)_{50}|$ (solid line) and $|(Xe)_{50}[Cl-I]^-(Xe)_{50}|$ (dotted line) with a solvent field of 0.004 au.

the one-sided chain model and the linear cluster model, molecular motions are expected to be quite extended even for the short-time dynamics of the heteronuclear diatom. Therefore, dynamic grids are used in these calculations.

3. Results

3.1. ICl$^-$ in a Linear-Chain Model. We investigated the dynamics of the model system $|(Ar)_{50}[Cl-I]^-(Ar)_{50}|$ and compared the results with those for the homonuclear case $|(Ar)_{50}[I-I]^-(Ar)_{50}|$. Figure 3 shows the internuclear distance of ICl$^-$ as a function of time after the photoexcitation. We considered different cases with increasing values for the solvent field. The dynamics of $|(Ar)_{50}[Cl-I]^-(Ar)_{50}|$ shows very early recombination characterized by the first decrease of the internuclear distance, and such a feature seems to have little dependence on the magnitude of the solvent field. After the initial decrease, the internuclear distance increases and shows oscillatory behavior whose frequency depends on the solvent field. The solvent dependence is shown in Figure 4 where the dynamics in two different solvents Ar and Xe are compared. The initial dynamics are similar, while the oscillations at later times show some differences.

From the comparison of the above results with those obtained in the previous study of the I$_2^-$ system, we note several interesting differences. The dynamics of ICl$^-$ indicate that the recombination occurs faster than in the I$_2^-$ case, which is consistent with the experimental findings.[17] As discussed before, we can consider three factors contributing to the difference between I$_2^-$ and ICl$^-$ recombination dynamics. Figure 5 shows the gradual change in the dynamics when we include the effects of the three factors. Starting with the I$_2^-$ dynamics, the first change is brought about when we switch the gas-phase potential energy surfaces for I$_2^-$ into those for ICl$^-$. The difference is mainly due to the change in excitation energy, 0.558 eV in I$_2^-$ to 0.502 eV in ICl$^-$, while the detailed shape of the PES makes a minor difference. Second, we incorporated the difference in the interaction of the solute with the solvent. The LJ parameters are changed to those for Cl−Ar pair at one side of the diatom. The solvent field is increased to 0.004 au in order to reflect the fact that the solvent configuration can be more asymmetric in the ICl$^-$ system. The effect of these changes makes the recombination more efficient. Finally, the mass for one of the diatom is changed to that for Cl atom. This change results in the occurrence of the very fast initial recombination noted before. More detailed information about the dynamics can be obtained by following the trajectories of the two atoms of the solute separately. In Figure 6, we plot the positions of I and Cl atoms along with the center of mass of the diatom for $|(Ar)_{50}[Cl-I]^-(Ar)_{50}|$ and $|(Xe)_{50}[Cl-I]^-(Xe)_{50}|$ systems. Because of the lighter mass, the motion of Cl is much faster than I. Initially, the Cl atom carries most of the excitation energy after the photoexcitation and it quickly collides with the solvent atom. The very fast initial recombination of ICl$^-$ is clearly the result of this motion of the Cl atom. In the Ar solvent, whose mass is similar to Cl, the energy transfer to the solvent atom is much efficient for Cl than I. The motion of the Cl atom shows rapid oscillation, while the overall motion of the I atom is slow except for the signature of oscillation due to collision with the Cl atom. It is also interesting to note that the center of mass of the solute is moving toward the I atom side because of the repeated collisions of the Cl atom with the I atom. When the solvent atoms are changed to Xe, the mass match is more favorable with the I atom than with the Cl atom. The energy transfer between I and Xe solvent atoms results in the characteristic oscillation in the position of the I atom. After rapid initial collisions with the solvent and the I

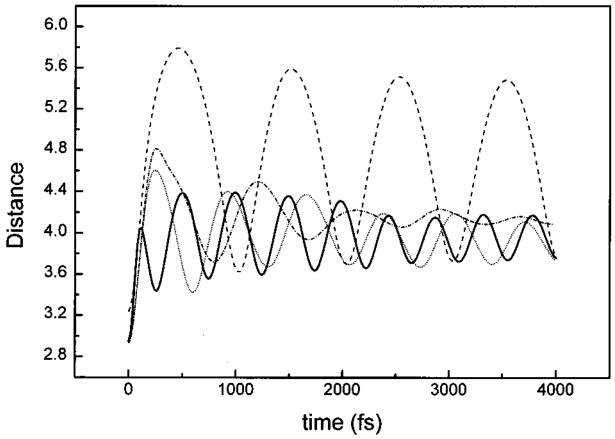

Figure 5. Averaged internuclear distances (in Å) showing the gradual change in the dynamics from the model system $|(Ar)_{50}[I-I]^-(Ar)_{50}|$ to $|(Ar)_{50}[Cl-I]^-(Ar)_{50}|$. Starting with the I$_2^-$ dynamics (dashed line), the first change is brought about when we switch the gas-phase potential energy surfaces for I$_2^-$ into those for ICl$^-$ (dot−dashed line). Second, we incoporated the difference in the interaction of the solute with the solvent including the increase in the solvent filed, 0.002 au → 0.004 au (dotted line). Finally, the mass of one of the diatoms is changed to that for a Cl atom (solid line).

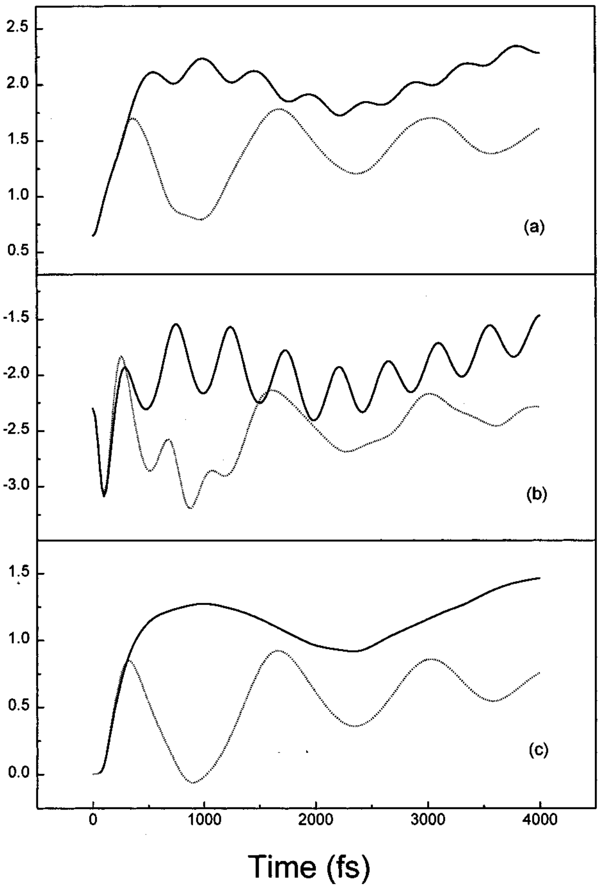

Figure 6. Absolute positions (in Å) of (a) the I atom, (b) the Cl atom, and (c) the center of mass of ICl^- in the model system $|(Ar)_{50}[Cl-I]^-(Ar)_{50}|$ (solid line) and $|(Xe)_{50}[Cl-I]^-(Xe)_{50}|$ (dotted line) with a solvent field of 0.004 au. The origin of the coordinate is taken to be the position of the center of mass of the diatom before the photoexcitation.

atom, the motion of the Cl atom follows that of the I atom. The position of the center of mass for the diatom also follows that of I, and the amount of shifting toward the heavier I side is smaller than in the case of the Ar solvent. This suggests that a larger fraction of the initial energy obtained from photoexcitation is available for the internal motion of the diatom in heavier Xe solvent.

3.2. ICl^- in a One-Sided Chain Model. When chemical reactions such as photodissociation are occurring in molecular clusters, the dynamics of the reaction is affected by the structural properties of clusters. Previous simulation studies of ionic molecular clusters have found that the minimum energy structures strongly depend on the size of the cluster, and for a small number of solvent atoms, one end of the chromophore is preferentially solvated.[12,14,15] Such asymmetric packing can produce an electric field that polarizes the charge distribution on the chromophore. Because of the initially asymmetric charge distribution of ICl^- molecule, Monte Carlo simulations of $ICl^-(CO_2)_n$ ions for small n show unequivocally a preferential packing of the solvent molecules around the smaller Cl atom.[37]

To model the asymmetric packing of the solvent atoms, we introduced a one-sided chain model. This corresponds to the removal of the right-side (I atom side) solvent atoms in Figure 1. As a comparison, we have also done calculations for the I_2^- case along with ICl^- using the one-sided chain model. In this model, the solute atoms are expected to travel in a much wider range; therefore, we used the dynamic grid method as introduced in the previous section. Figure 7 shows the time dependence of the internuclear distance for $|(Ar)_{50}[I-I]^-$ and $|(Ar)_{50}[Cl-I]^-$ with typical values of the solvent field. We have found that recombinations are occurring with the solvent atoms on only one side of the chain in both cases. Compared with the previous results from the linear-chain model with the solvent atoms on both sides of the solute, the internuclear distance of I_2^- is extended before the first recombination and the later oscillations show a longer wavelength with the amplitude much more reduced. Unlike the linear-chain model where the motions of both the diatom and the solvent atoms on each side are assumed to be symmetric, we need to follow the two solute atoms separately in the one-sided chain model. The absence of the solvent atoms on the right side allows the I atom to move a rather long distance, while the left-side I atom follows the other I atom until two atoms recombine after losing enough extra energy (Figure 8). Because of the asymmetry, the position of the center of mass for I_2^- is shifted toward the right.

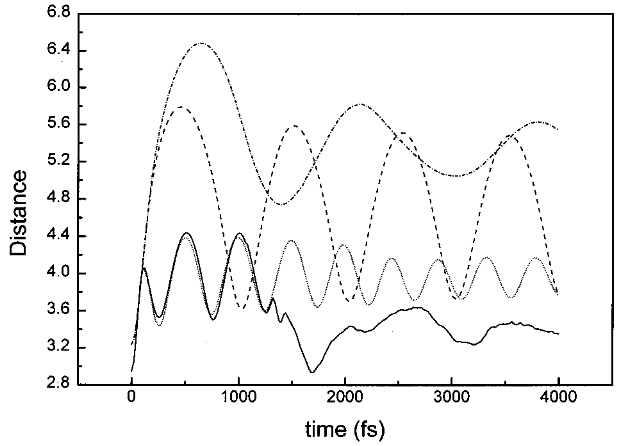

Figure 7. Comparison of the averaged internuclear distances (in Å) for the linear-chain model and the one-sided chain model. Four different model systems are considered: $|(Ar)_{50}[I-I]^-(Ar)_{50}|$ with $E = 0.002$ au (dashed line); $|(Ar)_{50}[I-I]^-$ with $E = 0.002$ au (dot−dashed line); $|(Ar)_{50}[Cl-I]^-(Ar)_{50}|$ with $E = 0.004$ au (dotted line); $|(Ar)_{50}[Cl-I]^-$ with $E = 0.004$ au (solid line).

For ICl^- in a one-sided chain, the initial dynamics is similar to the previous results with the linear-chain model. However, the internuclear distance does not show any regular oscillations while the extension of motion is much more reduced. Figure 9 displays the motions of I and Cl atoms along with the position of the center of mass for ICl^- in this case. The position of the I atom increases almost linearly with time up to $t \approx 1.3$ ps. After the initial collision with the solvent, the Cl atom catches up to the I atom, and eventually, the positions of the I and Cl atoms stay about constant for long times. Such behavior is also manifested in the position of the center of mass of the diatom. It is noted that the use of the dynamic grid method is essential in these calculations because the ranges of atomic movements are very large.

3.3. ICl^- in a Linear Cluster Model. The original linear-chain model can be considered to represent the situation where the solute is imbedded in rare-gas solid matrixes. It cannot describe fully the molecular clusters where the solvent atoms can be evaporated, resulting in rapid cooling of the system. We introduced a linear cluster model to mimic molecular clusters. The repulsive wall, to which the last solvent atom on each side of the linear chain is connected, is removed. As previously noted, the short-time dynamics should not be affected by this change. As shown in Figure 10, the dynamics of the $(Ar)_5[I-Cl]^-(Ar)_5$ cluster are almost the same as those of the linear-chain model for $|(Ar)_{50}$ $[I-Cl]^-$ $(Ar)_{50}|$ for $t < 4$ ps. Figure

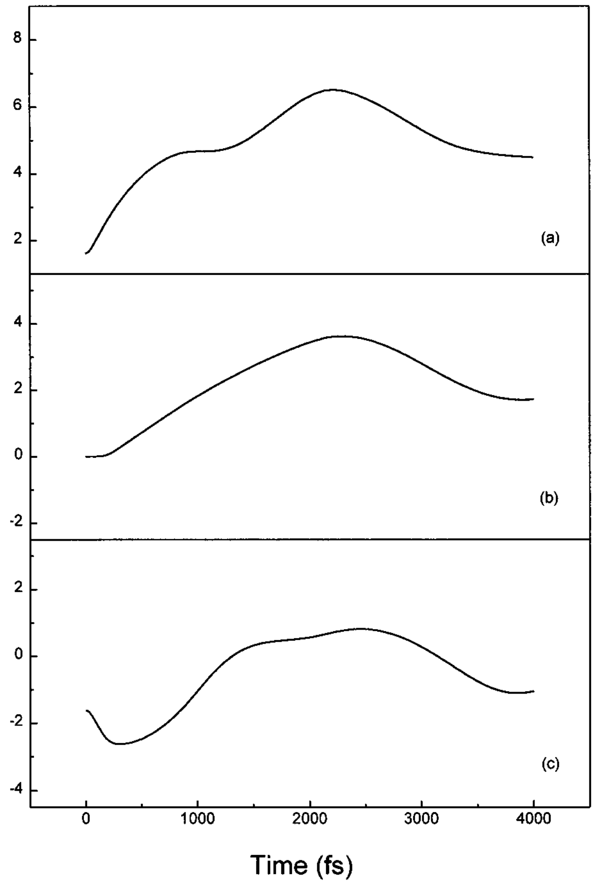

Figure 8. Absolute positions (in Å) of (a) the right-side I atom, (b) the center of mass of I_2^-, and (c) the left-side I atom in the model system $|(Ar)_{50}[I-I]^-$ with a solvent field of 0.002 au.

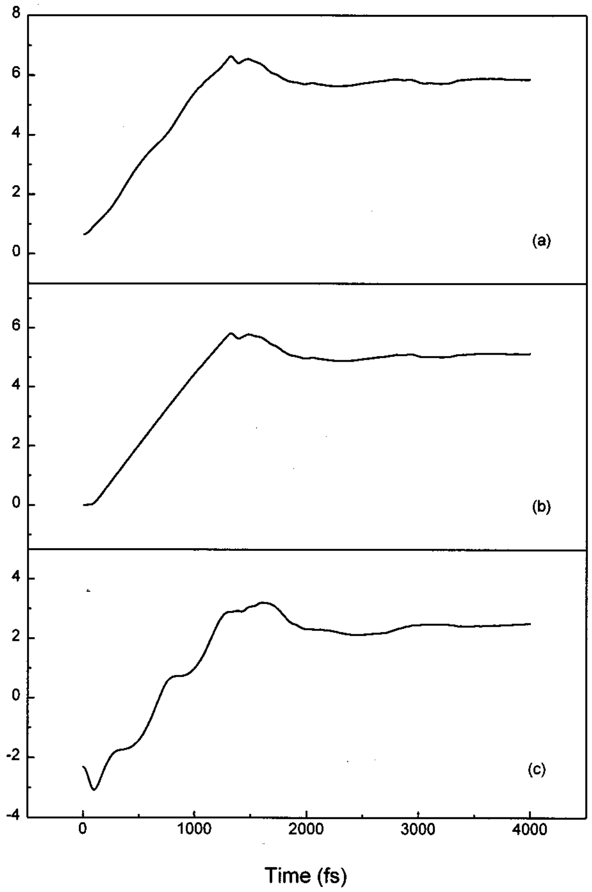

Figure 9. Absolute positions (in Å) of (a) the right-side I atom, (b) the center of mass of ICl$^-$, and (c) the left-side Cl atom in the model system $|(Ar)_{50}[Cl-I]^-$ with a solvent field of 0.004 au.

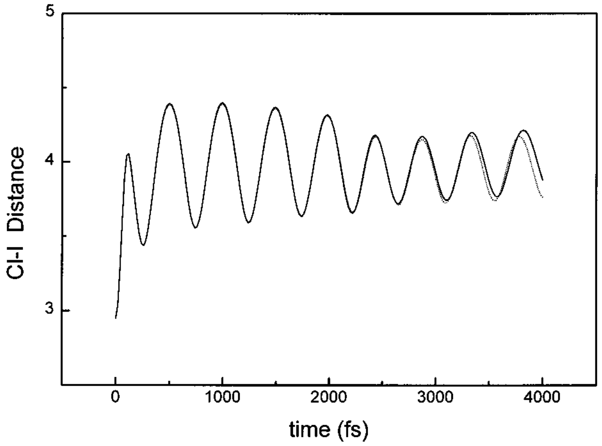

Figure 10. Comparison of the averaged internuclear Cl−I distances (in Å) for the linear-chain model system $|(Ar)_{50}[Cl-I]^-(Ar)_{50}|$ (dotted line) and the linear cluster model system $(Ar)_5[Cl-I]^-(Ar)_5$ (solid line) with a solvent field of 0.004 au.

11 shows the positions of the solvent atoms on each side of the linear cluster. It is clearly seen that the last solvent atoms evaporate at $t \approx 1$ ps as the energy is transferred to them. It can be argued that longer-time dynamics such as vibrational relaxation after recombination will be affected by the evaporation of solvent atoms. We have also considered a one-sided linear cluster model where only five atoms are connected to the Cl side of the ICl$^-$ molecule. The general behavior is much the same as in the $|(Ar)_{50}$ $[I-Cl]^-$ case, since important dynamics are occurring within 2 ps.

4. Conclusions

Theoretical studies of the photodissociation of ICl$^-$ in a linear-chain model of rare-gas solvent atoms have been carried out. We used a hybrid quantum/classical method in which the dynamics of the I and the Cl atoms are represented by the quantum mechanical wave packet propagation, while the motions of the solvent atoms are treated by classical trajectories. The effects of the electrostatic interactions due to solvent polarization and the initial charge asymmetry in the ICl$^-$ molecule are incorporated in the model by introducing an effective solvent field. To study the influence on the dynamics by the structural changes in the solvents, we also considered variations of the linear-chain model such as the one-sided chain model and the linear cluster model.

The theoretical model adopted in this study has obvious limitations due to its simplicity. As a 1D model, the linear-chain model cannot describe three-dimensional dynamics such as rotational motion, which might be important for the dissociation of ions in solution. The introduction of the solvent field to describe the polarization effect neglects the solvation dynamics in the local environments. In general, the linear-chain model will be valid for short-time dynamics. Despite such limitations, the present model is expected to contain enough of the physics to explain qualitatively some of the salient features observed in the real system. The extension of the model to more realistic situations will reveal the importance of the factors not included in the simpler model. The use of the quantum/classical method with the simplified system−bath coupling works well for the model system because the main concern is to treat the energy transfer between the solute and the solvent,

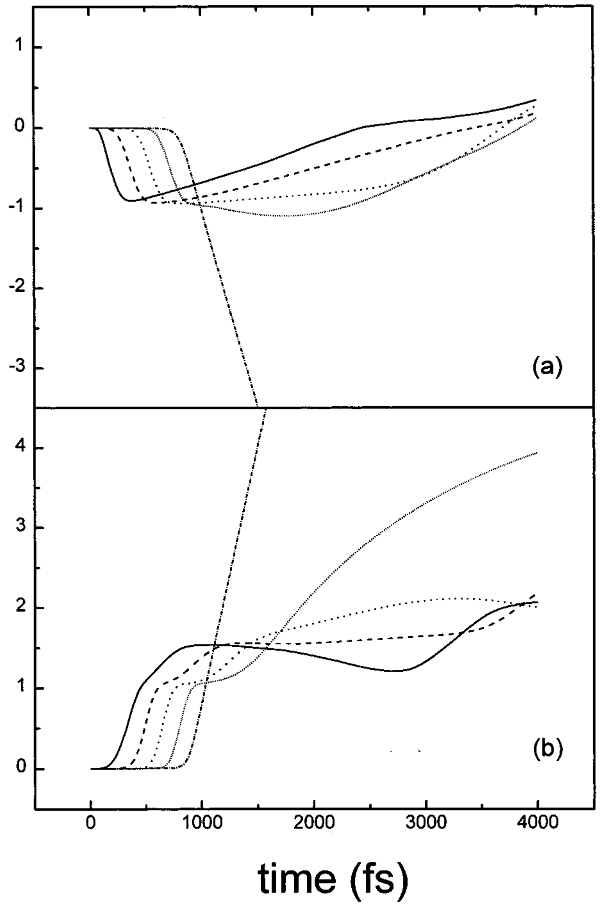

Figure 11. Absolute positions (in Å) of (a) the left-side solvent atoms and (b) the right-side solvent atoms in the linear cluster model system $(Ar)_5[Cl-I]^-(Ar)_5$ with a solvent field of 0.004 au. The solid line corresponds to the solvent atom closest to the solute atoms in both cases.

which is adequately described in the present scheme. Considering the rather large mass, even the dynamics of the solute can be described semiclassically, e.g., by using the Gaussian wave packets. Such a method will be useful when we extend the study to multidimensional systems for which only a few degrees of freedom can be treated exactly by quantum mechanics. Much more elaborate treatments of the couplings between the subsystems are needed if we consider the case where the dynamics of the solvents lead to transitions among quantum states of the solute.[14,15]

The dynamics of the heteronuclear diatomic ion (ICl^-) is much more complex compared with those for the homonuclear case (I_2^-). The photodissociation dynamics of ICl^- in a linear-chain model, $|(Ar)_{50}[Cl-I]^-(Ar)_{50}|$, show very fast initial recombination due to the motions of the lighter-mass Cl atom. Since the I and the Cl atoms show different behavior in the efficiency of the energy transfer to the solvent atoms, the detailed dynamics of ICl^- can show distinguishable solvent dependence. Another interesting feature is the shift of the center of mass of the diatom toward the heavier I atom side. It may be argued that such asymmetric motion of the heteronuclear diatom can lead to the instability of molecular clusters. To model the asymmetric packing of the solvent atoms, we introduced a one-sided chain model where the solvent atoms are present only on the Cl atom side of the diatom. It is found that recombinations are still occurring with the initial dynamics being similar to those with the linear-chain model. For longer-time dynamics, the internuclear distance does not show any regular oscillations while the extension of motion is much more reduced. It is noted that the use of the dynamic grid method is essential because the atomic motions are of much longer range. We have also considered a linear cluster model to mimic molecular clusters, where the solvent atoms can be evaporated. The general features of the short-time dynamics have not been affected by such changes. The model will be useful for much longer dynamics such as vibrational relaxation on the ground electronic state after recombination.

The results obtained in the present study provide plausible explanations for the experimental findings that caged products were observed with a very small number of solvent molecules in $ICl^-(CO_2)_n$ with $n = 2-6$, while $I_2^-(CO_2)_n$ first showed a caged product with $n \geq 5$. Since the initial recombination of ICl^- is found to be due to the fast motion and the efficient energy transfer of the Cl atom, only a few solvents, which will be located around the Cl atom because of the charge asymmetry of the bare ion, should be enough to induce the recombination. Moreover, the effect of solvent polarization is expected to be larger for the heteronuclear ICl^- case mainly because of the above-mentioned charge asymmetry. Such an effect is represented by the increased value for the solvent field in our model, which is found to enhance the recombination.

Experiments on the $ICl^-(CO_2)_n$ clusters showed that nonadiabatic processes accompanying charge switching played very important roles in the photodissociation and recombination dynamics of the system.[17,37] The theoretical model given in the present study cannot describe such nonadiabatic processes involving electronic transitions. Recently, we have proposed a one-electron model for the photodissociation and the recombination dynamics of the diatomic anion in condensed-phase environments. The main purpose of the study is to provide a minimal model for charge switching and nonadiabatic transitions involved in the dynamics of molecular ions. The model has been applied to the homonuclear I_2^- system, and interesting results have been obtained.[38] Further study is in progress to apply such a one-electron model to the heteronuclear ICl^- system, and we expect much complex behavior due to the initial charge asymmetry.

Acknowledgment. This work was supported by the Korean Science and Engineering Foundation (KOSEF) by Grant No. 961-0305-039-2 and through the Center for Molecular Catalysis at Seoul National University.

References and Notes

(1) Hynes, J. T. In *The Theory of Chemical Reaction*; Baer, M., Ed.; CRC Press: Boca Raton, FL, 1985; Vol. 4.

(2) *Reaction Dynamics in Clusters and Condensed Phases*; Jortner, J., Levine, R. D., Pullman, B., Eds.; Kluwer: Dordrecht, 1994.

(3) Johnson, A. E.; Levinger, N. E.; Barbara, P. F. *J. Phys. Chem.* **1992**, *96*, 7841.

(4) Kliner, D. A. V.; Alfano, J. C.; Barbara, P. F. *J. Chem. Phys.* **1993**, *98*, 5375.

(5) Alfano, J. C.; Kimura, Y.; Walhout, P. K.; Barbara, P. F. *Chem. Phys. Lett.* **1993**, *175*, 147.

(6) Benjamin, I.; Barbara, P. F.; Gertner, B. J.; Hynes, J. T. *J. Phys. Chem.* **1995**, *99*, 7557.

(7) Papanikolas, J. M.; Gord, J. R.; Levinger, N. E.; Ray, D.; Vorsa, V.; Lineberger, W. C. *J. Phys. Chem.* **1991**, *95*, 8028.

(8) Papanikolas, J. M.; Vorsa, V.; Nadal, M. E.; Campagnola, P. J.; Gord, J. R.; Lineberger, W. C. *J. Chem. Phys.* **1992**, *97*, 7002.

(9) Papanikolas, J. M.; Vorsa, V.; Nadal, M. E.; Campagnola, P. J.; Buchenau, H. K.; Lineberger, W. C. *J. Chem. Phys.* **1993**, *99*, 8733.

(10) Vorsa, V.; Campagnola, P. J.; Nandi, S.; Larsson, M.; Lineberger, W. C. *J. Chem. Phys.* **1996**, *105*, 2298.

(11) Vorsa, V.; Nandi, S.; Campagnola, P. J.; Larsson, M.; Lineberger, W. C. *J. Chem. Phys.* **1997**, *106*, 1402.

(12) Papanikolas, J. M.; Maslen, P. E.; Parson, R. *J. Chem. Phys.* **1995**, *102*, 2452.

(13) Greenblatt, B. J.; Zanni, M. T.; Neumark, D. M. *Science* **1997**, *276*, 1675.

(14) Batista, V. S.; Coker, D. F. *J. Chem. Phys.* **1997**, *106*, 7102.

(15) Faeder, J.; Delaney, N.; Maslen, P. E.; Parson, R. *Chem. Phys. Lett.* **1997**, *270*, 196.

(16) Parson, R.; Faeder, J. *Science* **1997**, *276*, 1660.

(17) Nadal, M. E.; Kleiber, P. D.; Lineberger, W. C. *J. Chem. Phys.* **1996**, *105*, 504.

(18) Ka, J.; Shin, S. *Chem. Phys. Lett.* **1997**, *269*, 227.

(19) Perera, L.; Amar, F. G. *J. Chem. Phys.* **1989**, *90*, 7354.

(20) Maslen, P. E.; Papanikolas, J. M.; Faeder, J.; Oneil, S. V.; Parson, R. *J. Chem. Phys.* **1994**, *101*, 5731.

(21) Papanikolas, J. M. Ph.D. Thesis, University of Colorado, 1994.

(22) Blake, N. P.; Srdanov, V.; Stucky, G. D.; Metiu, H. *J. Phys. Chem.* **1995**, *99*, 2127.

(23) Shin, S.; Metiu, H. *J. Chem. Phys.* **1995**, *102*, 9285.

(24) Messina, M.; Coalson, R. D. *J. Chem. Phys.* **1989**, *90*, 4015.

(25) Reichl, J. P.; Dielstler, D. J. *J. Chem. Phys.* **1976**, *64*, 2593.

(26) Roitberg, A. E.; Gerber, R. B.; Ratner, M. A. *J. Chem. Phys.* **1994**, *100*, 4355.

(27) Liu, L.; Guo, H. *Chem. Phys. Lett.* **1995**, *237*, 299.

(28) Liu, L.; Guo, H. *J. Chem. Phys.* **1995**, *103*, 7851.

(29) Liu, L.; Guo, H. *J. Chem. Phys.* **1996**, *104*, 528.

(30) Maslen, P. E.; Faeder, J.; Parson, R. *Chem. Phys. Lett.* **1996**, *263*, 63.

(31) Schatz, G. C.; Ratner, M. A. *Quantum Mechanics in Chemistry*; Prentice Hall: Englewood Cliffs, NJ, 1993.

(32) Feit, M. D.; Fleck, J. A., Jr.; Steiger, A. *J. Comput. Phys.* **1982**, *47*, 412.

(33) Kosloff, R. *J. Phys. Chem.* **1988**, *92*, 2087.

(34) Allen, M. P.; Tildesley, D. J. *Computer Simulation of Liquids*; Clarendon Press: Oxford, 1987.

(35) Kosloff, R. In *Dynamics of Molecules and Chemical Reactions*; Wyatt, R. E., Zhang, J. Z. H., Eds.; Marcel Dekker: New York, 1996.

(36) Leforestier, C. *Chem. Phys.* **1984**, *87*, 241.

(37) Lineberger, W. C.; Nadal, M. E.; Campagnola, P. J.; Vorsa, V.; Kleiber, P. D.; Papanikolas, J. M.; Maslen, P. E.; Faeder, J.; Parson, R.; Poplawski, O. In *Proceedings of The Robert A. Welch Foundation, 38th Conference on Chemical Research: Chemical Dynamics of Transient Species*; R. A. Welch Foundation: Houston, TX, 1994; Vol. 38, pp 175–184.

(38) Ka, J.; Shin, S. Submitted for publication.